

Supplement of

Modeling studies for SOA formation from α -pinene ozonolysis

Kathrin Gatzsche¹, Yoshiteru Iinuma^{1,*}, Andreas Tilgner¹, Anke Mutzel¹, Torsten Berndt¹, and Ralf Wolke¹

¹Leibniz Institute for Tropospheric Research, Leipzig, Germany

*now at: Okinawa Institute of Science and Technology Graduate University (OIST), Okinawa, Japan

Correspondence to: K. Gatzsche (gatzsche@tropos.de)

1 Gas-phase chemistry mechanism for α -pinene oxidation

Table S1: Reaction mechanism for the degradation of α -pinene according to Chen and Griffin (2005) updated by rate constants from MCM and HOM yields.

#	Reactants	Products	Rate constant in $\text{cm}^3 \text{molecule}^{-1} \text{s}^{-1}$	Ref.
1a	APIN + OH	$\rightarrow \text{RO}_2\text{101} + \text{RO}_2\text{T}$	$1.21\text{E-11} \times \exp(444/T)$	1, 6
1b	APIN + OH	$\rightarrow 0.961 \text{RO}_2\text{101} + 0.961 \text{RO}_2\text{T} + 0.024 \text{HOM}^\dagger$	$1.21\text{E-11} \times \exp(444/T)$	1, 6
2	APIN + NO ₃	$\rightarrow \text{RO}_2\text{102} + \text{RO}_2\text{T}$	$1.2\text{E-12} \times \exp(490/T)$	1, 6
3a	APIN + O ₃	$\rightarrow 0.2 \text{RO}_2\text{103} + 0.2 \text{CO} + 0.8 \text{OH} + 0.05 \text{UR101} + 0.15 \text{PINA} + 0.15 \text{H}_2\text{O}_2 + 0.33 \text{RO}_2\text{104} + 0.27 \text{RO}_2\text{105} + 0.8 \text{RO}_2\text{T}$	$8.05\text{E-16} \times \exp(640/T)$	1, 6
3b	APIN + O ₃	$\rightarrow 0.1932 \text{RO}_2\text{103} + 0.1932 \text{CO} + 0.7728 \text{OH} + 0.0483 \text{UR101} + 0.1449 \text{PINA} + 0.1449 \text{H}_2\text{O}_2 + 0.31878 \text{RO}_2\text{104} + 0.26082 \text{RO}_2\text{105} + 0.034 \text{HOM}^\dagger$	$8.05\text{E-16} \times \exp(640/T)$	1, 6
4	APIN + O ₃ PX	$\rightarrow 0.75 \text{UR103} + 0.25 \text{NOPI}$	3.2E-11	2
5	RO ₂ 101 + NO	$\rightarrow 0.2 \text{AP101} + 0.6 \text{PINA} + 0.8 \text{HO}_2 + 0.2 \text{KETH} + 0.2 \text{HCHO}$	$8.8\text{E-13} \times \exp(180.2/T)$	2
6	RO ₂ 101 + RO ₂ T	$\rightarrow 0.7 \text{PINA} + \text{HO}_2 + 0.3 \text{UR107} + \text{O}_2$	$1.82\text{E-13} \times \exp(416/T)$	2
7	RO ₂ 101 + HO ₂	$\rightarrow 0.8 \text{PINA} + 0.2 \text{KETH} + 0.2 \text{HCHO} + \text{OOH1}$	$4.1\text{E-13} \times \exp(790/T)$	2
8	RO ₂ 102 + NO	$\rightarrow 0.6 \text{PINA} + 1.825 \text{NO}_2 + 0.175 \text{AP102} + 0.225 \text{KETH} + 0.225 \text{HCHO} + 0.4 \text{HO}_2$	$8.8\text{E-13} \times \exp(180.2/T)$	2
9	RO ₂ 102 + RO ₂ T	$\rightarrow 0.795 \text{PINA} + 0.795 \text{NO}_2 + 0.135 \text{AP101} + 0.07 \text{AP102} + \text{O}_2$	$1.82\text{E-13} \times \exp(416/T)$	2

10	$\text{RO}_2102 + \text{HO}_2$	$\rightarrow 0.6 \text{ PINA} + 0.825 \text{ NO}_2 + 0.175 \text{ AP102} + 0.225 \text{ HCHO} + 0.225 \text{ HO}_2 + 0.175 \text{ OOH1} + 0.825 \text{ OOH2}$	$4.1\text{E}-13 \times \exp(790/T)$	2
11	$\text{RO}_2103 + \text{NO}$	$\rightarrow 0.38 \text{ AP103} + 0.62 \text{ NRPA} + 0.62 \text{ HO}_2 + 0.62 \text{ NO}_2$	$1.05\text{E}-12 \times \exp(180.2/T)$	2, a
12	$\text{RO}_2103 + \text{RO}_2\text{T}$	$\rightarrow \text{NRPA} + \text{HO}_2 + \text{O}_2$	$1.82\text{E}-13 \times \exp(416/T)$	2
13	$\text{RO}_2103 + \text{HO}_2$	$\rightarrow \text{NRPA} + \text{OOH1}$	$4.1\text{E}-13 \times \exp(790/T)$	2
14	$\text{RO}_2104 + \text{NO}$	$\rightarrow \text{NO}_2 + \text{RO}_2108 + \text{RO}_28$	$8.8\text{E}-13 \times \exp(180.2/T)$	2
15	$\text{RO}_2104 + \text{RO}_2\text{T}$	$\rightarrow 0.7 \text{ RO}_2108 + 0.7 \text{ RO}_28 + 0.3 \text{ RP102} + \text{O}_2$	$1.82\text{E}-13 \times \exp(416/T)$	2
16	$\text{RO}_2104 + \text{HO}_2$	$\rightarrow \text{RO}_2108 + \text{RO}_28 + \text{OOH2}$	$4.1\text{E}-13 \times \exp(790/T)$	2
17	$\text{RO}_2105 + \text{NO}$	$\rightarrow \text{HCHO} + \text{NO}_2 + \text{RO}_2109$	$8.8\text{E}-13 \times \exp(180.2/T)$	2
18	$\text{RO}_2105 + \text{RO}_2\text{T}$	$\rightarrow 0.8 \text{ HCHO} + 0.8 \text{ RO}_2109 + 0.10 \text{ UR105} + 0.05 \text{ RP103} + 0.05 \text{ UR108} + \text{O}_2$	$1.82\text{E}-13 \times \exp(416/T)$	2
19	$\text{RO}_2105 + \text{HO}_2$	$\rightarrow \text{HCHO} + \text{RO}_2109 + \text{OOH2}$	$4.1\text{E}-13 \times \exp(790/T)$	2
20	$\text{PINA} + h\nu$	$\rightarrow \text{CO} + \text{HO}_2 + \text{RO}_2103$	Photolysis MCM*	6, 7
21	$\text{PINA} + \text{OH}$	$\rightarrow 0.8 \text{ RO}_2106 + 0.2 \text{ RO}_2104 + \text{H}_2\text{O}$	$9.1\text{E}-11$	4
22	$\text{PINA} + \text{NO}_3$	$\rightarrow \text{RO}_2106 + \text{HNO}_3$	$5.4\text{E}-14$	4
23	$\text{RO}_2106 + \text{NO}$	$\rightarrow \text{RO}_2103 + 0.8 \text{ CO}_2 + \text{O}_2$	$1.11\text{-}11 \times \exp(180.2/T)$	2
24	$\text{RO}_2106 + \text{NO}_2 + \text{M}$	$\rightarrow \text{PAN101} + \text{M}$	Refer to reference	3
25	PAN101	$\rightarrow \text{RO}_2106 + \text{NO}_2$	Refer to reference	3
26	$\text{RO}_2106 + \text{RO}_2\text{T}$	$\rightarrow 0.2 \text{ UR101} + 0.8 \text{ RO}_2103 + 0.8 \text{ CO}_2 + \text{O}_2$	$5.0\text{E}-12$	2
27	$\text{RO}_2106 + \text{HO}_2$	$\rightarrow 0.2 \text{ UR101} + \text{O}_3$	$4.3\text{E}-13 \times \exp(1040/T)$	2
28	$\text{NRPA} + h\nu$	$\rightarrow \text{CO} + \text{HO}_2 + \text{RO}_2108$	Photolysis MCM*	6, 7
29	$\text{NRPA} + \text{OH}$	$\rightarrow 0.8 \text{ RO}_2107 + 0.2 \text{ RO}_2104 + \text{H}_2\text{O}$	$9.1\text{E}-11$	4
30	$\text{NRPA} + \text{NO}_3$	$\rightarrow \text{RO}_2107 + \text{HNO}_3$	$5.4\text{E}-14$	4
31	$\text{RO}_2107 + \text{NO}$	$\rightarrow \text{NO}_2 + \text{CO}_2 + \text{RO}_2108$	$1.11\text{-}11 \times \exp(180.2/T)$	2
32	$\text{RO}_2107 + \text{NO}_2 + \text{M}$	$\rightarrow \text{PAN102} + \text{M}$	Refer to reference	3
33	PAN102	$\rightarrow \text{RO}_2107 + \text{NO}_2$	Refer to reference	3
34	$\text{RO}_2107 + \text{RO}_2\text{T}$	$\rightarrow 0.2 \text{ UR102} + 0.8 \text{ CO}_2 + 0.87, \text{RO}_2108 + \text{O}_2$	$5.0\text{E}-12$	2
35	$\text{RO}_2107 + \text{HO}_2$	$\rightarrow \text{UR102} + \text{O}_3$	$4.3\text{E}-13 \times \exp(1040/T)$	2
36	$\text{RO}_2108 + \text{NO}$	$\rightarrow 0.35 \text{ AP104} + 0.65 \text{ KETH} + 0.65 \text{ NO}_2 + 0.65 \text{ HO}_2$	$1.24\text{E}-12 \times \exp(180.2/T)$	2, a
37	$\text{RO}_2108 + \text{RO}_2\text{T}$	$\rightarrow \text{KETH} + \text{HO}_2 + \text{O}_2$	$1.82\text{E}-13 \times \exp(416/T)$	2
38	$\text{RO}_2108 + \text{HO}_2$	$\rightarrow \text{KETH} + \text{OOH1}$	$4.1\text{E}-13 \times \exp(790/T)$	2
39	$\text{RO}_2109 + \text{NO}$	$\rightarrow \text{CO}_2 + \text{NO}_2 + \text{RO}_2108$	$1.11\text{-}11 \times \exp(180.2/T)$	2
40	$\text{RO}_2109 + \text{NO}_2 + \text{M}$	$\rightarrow \text{PAN103} + \text{M}$	Refer to reference	3
41	PAN103	$\rightarrow \text{RO}_2109 + \text{NO}_2$	Refer to reference	3
42	$\text{RO}_2109 + \text{RO}_2\text{T}$	$\rightarrow 0.3 \text{ RP101} 0.1 \text{ UR104} + 0.6 \text{ CO}_2 + 0.6 \text{ RO}_2108 + \text{O}_2$	$5.0\text{E}-12$	2

43	$\text{RO}_2109 + \text{HO}_2$	$\rightarrow \text{UR104} + \text{O}_2$	$4.3\text{E}-13 \times \exp(1040/T)$	2
44	$\text{AP101} + \text{OH}$	$\rightarrow \text{PINA} + \text{NO}_2 + \text{H}_2\text{O}$	5.63E-12	5
45	$\text{AP102} + \text{OH}$	$\rightarrow \text{RO}_2108 + \text{NO}_2 + \text{H}_2\text{O}$	6.86E-12	5
46	$\text{AP103} + \text{OH}$	$\rightarrow \text{NRPA} + \text{NO}_2 + \text{H}_2\text{O}$	2.53E-12	5
47	$\text{AP104} + \text{OH}$	$\rightarrow \text{KETH} + \text{NO}_2 + \text{H}_2\text{O}$	2.02E-12	5
48	$\text{RP101} + \text{OH}$	$\rightarrow \text{UR104} + \text{O}_3 - \text{HO}_2$	2.62E-11	5
49	$\text{RP102} + \text{OH}$	$\rightarrow \text{UR106} + \text{O}_3 - \text{HO}_2$	2.36E-11	5
50	$\text{RP103} + \text{OH}$	$\rightarrow \text{UR105} + \text{O}_3 - \text{HO}_2$	2.66E-11	5

[†] Reactions updated by HOM yields according to Berndt et al. (2016) utilized for cases 5a and 5b of Table 1

a) Yields calculated according to Arey et al. (2001)

References: 1) Atkinson (1997); 2) Jenkin et al. (1997); 3) Griffin et al. (2002); 4) Glasius et al. (1997); 5) Kwok and Atkinson (1995); 6) <http://mcm.leeds.ac.uk/MCM/>; 7) Saunders et al. (2003)

* Photolysis according to Saunders et al. (2003) with $J = l(\cos(\chi))^m \exp(-n \sec \chi)$ with χ the solar zenith angle; $l = 2.792\text{E}-05$; $m = 0.805$; $n = 0.338$.

Table S2: Abbreviations and full names of the chemical species included in the α -pinene oxidation mechanism.

Term	Description
Reactive, fully integrated species	
APIN	α -pinene
PINA	pinonaldehyde
NRPA	norpinonaldehyde
AP101	2-nitro-3-hydroxy-pinane
AP102	2-nitro-3-oxo-pinane
AP103	2,2-dimethyl-3-acetyl-cyclobutyl-methyl-nitrate
AP104	2,2-dimethyl-3-acetyl-cyclobutyl-nitrate
HOM	highly oxidized organic compound
PAN101	peroxy 2,2-dimethyl-3-acetyl-cyclobutyl-acetyl-nitrate
PAN102	peroxy 2,2-dimethyl-3-acetyl-cyclobutyl-formyl-nitrate
PAN103	peroxy 2,2-dimethyl-3-formylmethyl-cyclobutyl-formyl-nitrate
RP101	pinalic-3-acid
RP102	1-hydroxy-pinonaldehyde
RP103	10-hydroxy-pinonaldehyde
Nonreacting, fully integrated species	

- UR101 pinonic acid
UR102 norpinonic acid
UR103 2,3-pinane-epoxide
UR104 pinic acid
UR105 10-hydroxy-pinonic acid
UR106 1-hydroxy-pinonic acid
UR107 2,3-dihydroxy-pinane
UR108 2-(2,2-dimethyl-3-formylmethyl-cyclobutyl)-2-keto-acetaldehyde

Reactive, organic pseudo-steady species

- RO₂101 hydroxy alkyl peroxy radical from oxidation of α -pinene (2-peroxy-3-hydroxy-pinane)
RO₂102 nitrato alkyl peroxy radical from oxidation of α -pinene (65 % is 2-peroxy-3-nitrito-pinane, 35 % is 2-nitroso-3-peroxy-pinane)
RO₂103 cyclic keto alkyl peroxy radical from oxidation of α -pinene (C₄ cycle, 1-methyl peroxy, 2,2-dimethyl, 3-acetyl)
RO₂104 cyclic keto aldehydic peroxy radical from oxidation of α -pinene (C₄ cycle, 1-peroxy, 1-acetyl, 2,2-dimethyl, 3-formylmethyl)
RO₂105 cyclic keto alkyl peroxy radical from oxidation of α -pinene (C₄ cycle, 1-(1-keto-ethyl peroxy), 2,2-dimethyl, 3-formylmethyl)
RO₂106 acyl peroxy radical from aldehydic H abstraction of pinonaldehyde
RO₂107 acyl peroxy radical from aldehydic H abstraction of norpinonaldehyde
RO₂108 cyclic keto alkyl peroxy radical from oxidation of α -pinene (C₄ cycle, 1-peroxy, 2,2-dimethyl, 3-acetyl)
RO₂109 acyl peroxy radical from oxidation of α -pinene (C₄ cycle, 1-formyl peroxy, 2,2-dimethyl, 3-formylmethyl)
-

Table S3: Considered particle phase reactions for α -pinene oxidized products required for the kinetic approach and added to the reaction mechanism presented in Table S1.

#	Reactants		Products	Rate constant in s^{-1}
51	pPINA	\rightarrow	rPINA	$1 - 10^{-6}$
52	pRP101	\rightarrow	rRP101	$1 - 10^{-6}$
53	pUR104	\rightarrow	rUR104	$1 - 10^{-6}$
54	pNRPA	\rightarrow	rNRPA	$1 - 10^{-6}$
55	pRP102	\rightarrow	rRP102	$1 - 10^{-6}$
56	pRP103	\rightarrow	rRP103	$1 - 10^{-6}$
57	pUR101	\rightarrow	rUR101	$1 - 10^{-6}$
58	pUR102	\rightarrow	rUR102	$1 - 10^{-6}$
59	pUR105	\rightarrow	rUR105	$1 - 10^{-6}$
60	pUR106	\rightarrow	rUR106	$1 - 10^{-6}$
61	pAP101	\rightarrow	rAP101	$1 - 10^{-6}$
62	pAP102	\rightarrow	rAP102	$1 - 10^{-6}$
63	pPAN101	\rightarrow	rPAN101	$1 - 10^{-6}$
64	pPAN102	\rightarrow	rPAN102	$1 - 10^{-6}$
65	pPAN103	\rightarrow	rPAN103	$1 - 10^{-6}$
66	pNOPI	\rightarrow	rNOPI	$1 - 10^{-6}$
67	rPINA	\rightarrow	pPINA	$1 - 10^{-6}$
68	rRP101	\rightarrow	pRP101	$1 - 10^{-6}$
69	rUR104	\rightarrow	pUR104	$1 - 10^{-6}$
70	rNRPA	\rightarrow	pNRPA	$1 - 10^{-6}$
71	rRP102	\rightarrow	pRP102	$1 - 10^{-6}$
72	rRP103	\rightarrow	pRP103	$1 - 10^{-6}$
73	rUR101	\rightarrow	pUR101	$1 - 10^{-6}$
74	rUR102	\rightarrow	pUR102	$1 - 10^{-6}$
75	rUR105	\rightarrow	pUR105	$1 - 10^{-6}$
76	rUR106	\rightarrow	pUR106	$1 - 10^{-6}$
77	rAP101	\rightarrow	pAP101	$1 - 10^{-6}$
78	rAP102	\rightarrow	pAP102	$1 - 10^{-6}$
79	rPAN101	\rightarrow	pPAN101	$1 - 10^{-6}$

80	rPAN102	\rightarrow	pPAN102	$1 - 10^{-6}$
81	rPAN103	\rightarrow	pPAN103	$1 - 10^{-6}$
82	rNOPI	\rightarrow	pNOPI	$1 - 10^{-6}$

Remarks: Reactions 67–82 describe the backward reactions considered for the sensitivity studies.

Table S4. Estimated vapor pressure of HOMs at 295 K.

Substance	SIMPOL	COSMO-RS*	EVAPORATION
HO-C ₁₀ H ₁₅ (OO)(OOH) ₂	8.82E-11	9.9E-11	5.52E-13
HO-C ₁₀ H ₁₅ (OO)(OOH)ONO ₂	1.59E-10	8.1E-10	7.00E-11
HO-C ₁₀ H ₁₅ (OO)(OOH)OH	1.58E-10	2.0E-10	6.23E-12

* Estimates of COSMO-RS according to Berndt et al. (2016)

2 Results

2.1 Impact of the particle phase diffusion coefficient D_b on SOA formation

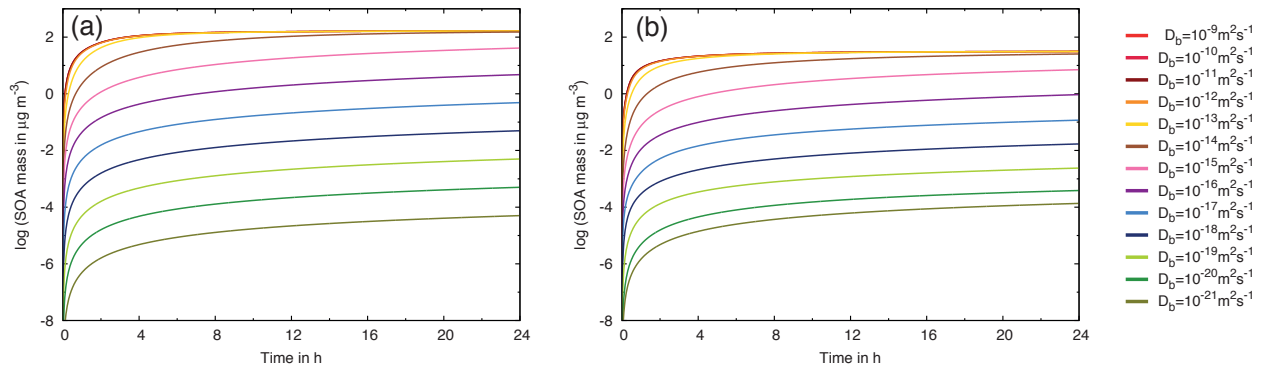


Figure S1. Simulated SOA mass for the variation of the bulk particle diffusion coefficient in the range of $D_b: 10^{-9} \text{ m}^2 \text{s}^{-1} - 10^{-21} \text{ m}^2 \text{s}^{-1}$ (case 1 of Table 1) in logarithmic scale for a) $k_c = 1 \text{ s}^{-1}$ and b) $k_c = 10^{-6} \text{ s}^{-1}$.

2.2 Impact of the mass accommodation coefficient α on SOA formation

An additional parameter influencing the SOA formation represents the mass accommodation coefficient (see Appendix A), which is defined as the probability to incorporate a molecule penetrating the particle phase boundary in the condensed phase without inducing the direct emission of a molecule of an identical type (Seinfeld and Pandis, 2006). This subsection investigates the sensitivity of SOA formation on the applied mass accommodation coefficient α . In the literature different values for the mass accommodation coefficient have been proposed for the uptake of organic compounds in organic particles/ on organic surfaces. Experimental studies show different results than model studies. Saleh et al. (2012) propose an approximate value of $\alpha = 0.4$ from evaporation studies for semi-volatile organic aerosols. In the review of Davidovits et al. (2006) concerning measured mass accommodation coefficients, the uptake values of organic species (e.g. acetic acid, α -pinene, γ -terpinene, p-cymene, and 2-methyl-2-hexanol) on 1-octanol surfaces are summarized. The mass accommodation coefficients are in the range of 0.12 and 0.4 for 265 K, whereby for α -pinene only a lower limit with $\alpha > 0.1$ is given. Moreover, Julin et al. (2014) have been combined expansion chamber measurements and molecular dynamics simulations for the determination of the mass accommodation coefficient, where bulk and surface mass accommodation coefficients have been distinguished. The probed organic substances were in liquid, semi-solid or solid phase state. Julin et al. (2014) report surface accommodation coefficients near unity ($0.96 \leq \alpha_s \leq 1$) and the bulk mass accommodation coefficients in the range of $0.14 \leq \alpha_b \leq 1$. Whereby, Julin et al. (2014) state that the conservative lower limits of the bulk mass accommodation coefficients are not very likely, due to the short simulation time scales and near unity values might be consistent with the surface mass accommodation coefficient. Additionally, the lower limit for the bulk mass accommodation coefficient assumes that adsorbed molecules will never enter

the particle bulk, and therefore, only absorbed molecules reach the particle bulk.

According to this wide spread of reported values of the mass accommodation coefficient, we varied α from 1 to 10^{-2} for all organic compounds. Further, we investigated these sensitivity studies for different bulk particle phase diffusion coefficients and pseudo-first-order rate constants of particle reactions (see model case 3a and 3b in Table 1). Fig.S2 shows the results of SOA

5 formation for different mass accommodation coefficients and fast particle phase reactions ($k_c = 1$). The SOA mass is highest for $\alpha = 1$. For liquid aerosol particles the simulated SOA mass for $\alpha = 10^{-1}$ in fact leads to about 97 % of the formed SOA mass of the model run using $\alpha = 1$ (see Fig. S2a). For $\alpha = 10^{-2}$ the SOA mass is markedly reduced showing only about 45 % of the maximal simulated value. For nearly semi-solid aerosol particles ($D_b = 10^{-14} \text{ m}^2 \text{ s}^{-1}$, see Fig. S2b) the SOA formation for $\alpha = 10^{-1}$ is reduced to 15 % of the SOA mass for the simulation with $\alpha = 1$. This demonstrates that the effect on the
10 SOA formation is more substantial when a reduced number of molecules is transferred into the particle surface/bulk and the particle phase diffusion is slower. For semi-solid aerosols ($D_b = 10^{-18} \text{ m}^2 \text{ s}^{-1}$) the simulation results are similar to those for nearly semi-solid particles with $D_b = 10^{-14} \text{ m}^2 \text{ s}^{-1}$ and are thus not presented. For moderate particle phase reactions the SOA formation for the reduced mass accommodation coefficients performs in the same way as for fast reactions (see Fig. S2c and S2d).

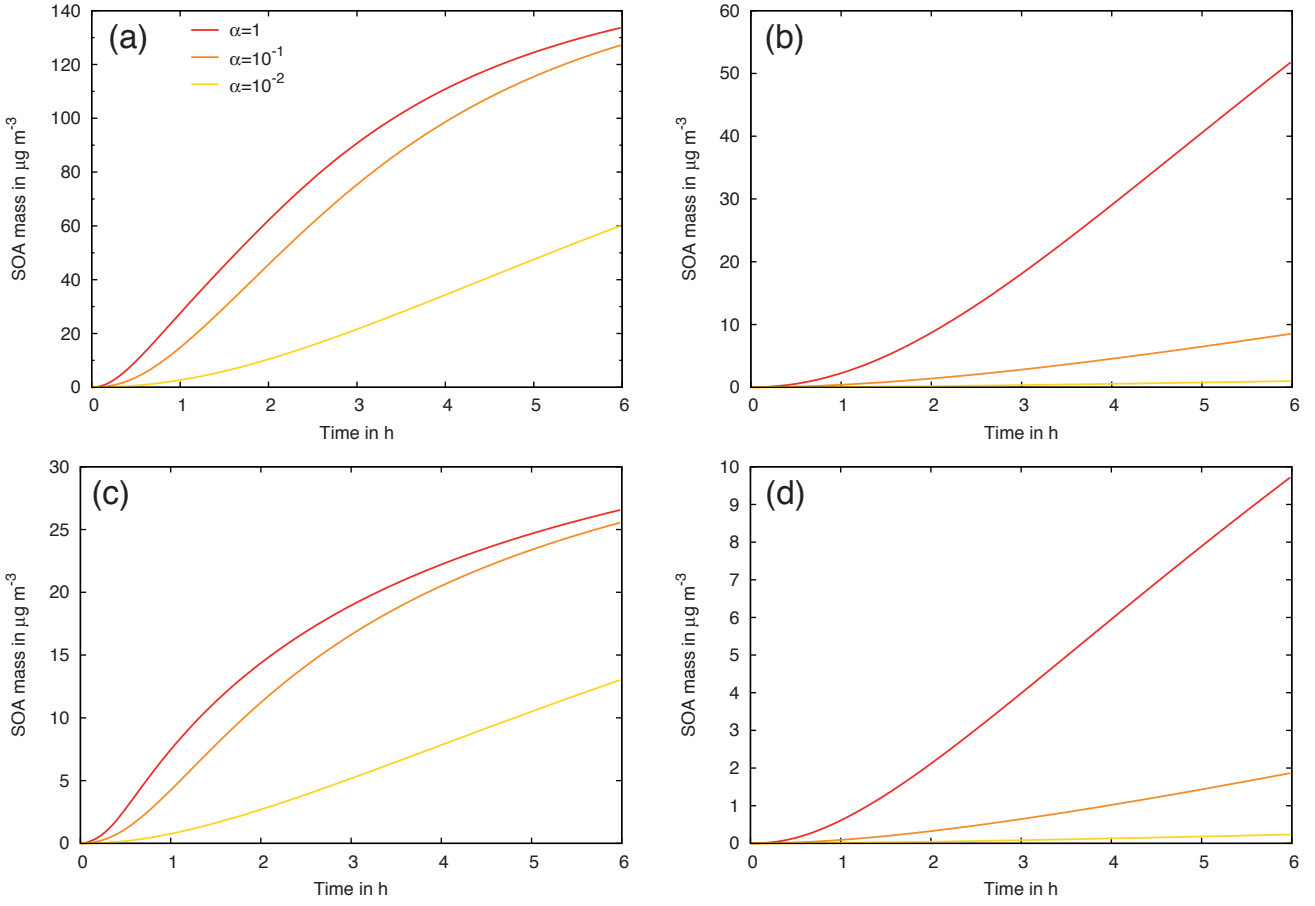


Figure S2. Simulated SOA mass for different mass accommodation coefficients for $k_c = 1$ (model case 3a of Table 1) using bulk particle diffusion coefficients for a) liquid ($D_b = 10^{-12} \text{ m}^2 \text{ s}^{-1}$) and b) the transition between liquid and semi-solid ($D_b = 10^{-14} \text{ m}^2 \text{ s}^{-1}$) aerosol particles and for $k_c = 10^{-4}$ (model case 3b of Table 1) using bulk particle diffusion coefficients for c) liquid ($D_b = 10^{-12} \text{ m}^2 \text{ s}^{-1}$) and d) the transition between liquid and semi-solid ($D_b = 10^{-14} \text{ m}^2 \text{ s}^{-1}$) aerosol particles.

2.3 Impact of the initial particle phase organic mass concentration OM_0 on SOA formation

Organic material in the aerosol phase serves as an absorptive medium for organic gaseous compounds (see Eq. 4). In order to investigate the dependency of the SOA formation from the initial organic aerosol mass OM_0 , the initial value has been varied from 10^{-5} to $5.8 \times 10^{-2} \text{ g g}^{-1}$ (see Table 1, model study 5). Fig. S3 shows the results for the variation of the initial organic mass for liquid and semi-solid particles, whereby $k_c = 10^{-1} \text{ s}^{-1}$ is held constant. For liquid particles (Fig. S3a) the initial organic mass has a marginal influence on the formed SOA mass because overall high organic mass concentrations occur for this parameter setup. For an intermediate diffusion coefficient $D_b = 10^{-14} \text{ m}^2 \text{ s}^{-1}$ the effect of the initial organic mass is also insignificant (not shown here). For the semi-solid particles (Fig. S3b) the initial organic mass influences noticeably the formed

SOA mass. However, the total SOA mass is very low and, therefore, the relative influence of the initial organic aerosol mass is increased. The variation of the initial organic particle concentration mass has no significant influence on the formed SOA mass for aerosol particles where effective SOA formation occurs. Additionally, it is noted that a small initial organic particle mass is required for the numerical computation of the equilibrium term, otherwise the partitioning term cannot be calculated (see Eq. 4). This approach is appropriate under ambient conditions.

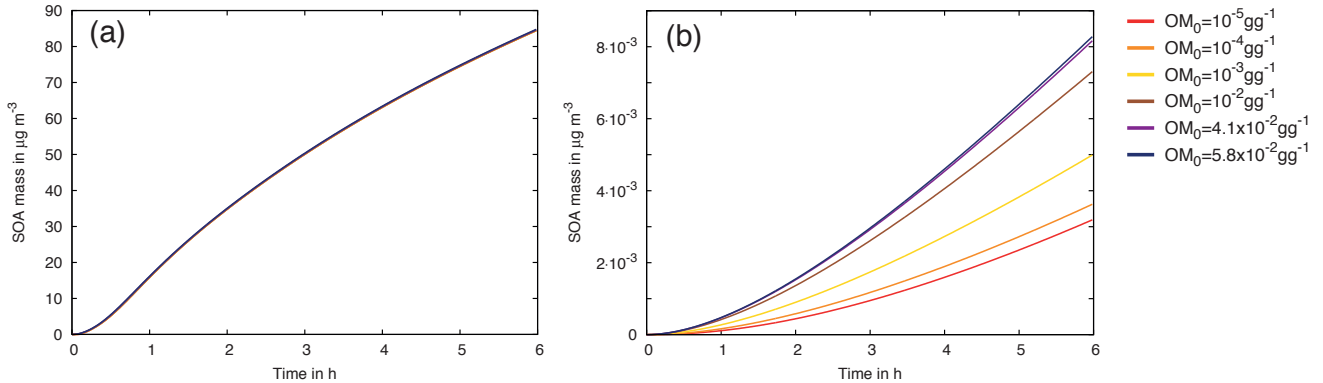


Figure S3. Simulated SOA mass formation for different initial particle phase organic mass concentrations OM_0 (model case 5 of Table 1) using diffusion coefficients of a) liquid ($D_b = 10^{-12} \text{ m}^2 \text{ s}^{-1}$) and b) semi-solid ($D_b = 10^{-18} \text{ m}^2 \text{ s}^{-1}$) aerosol particles.

2.4 Influence of the particle radius r_p on SOA formation

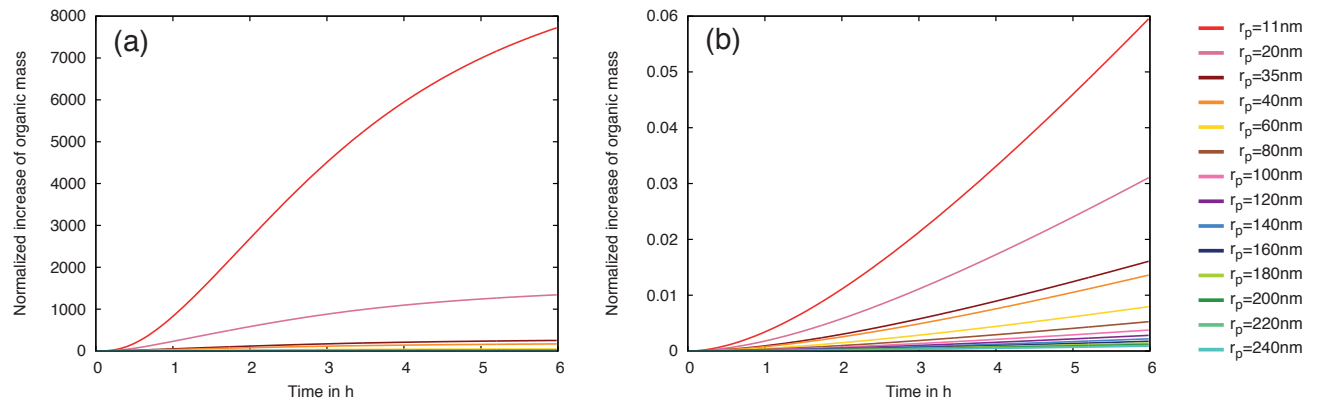


Figure S4. Normalized increase of organic mass, which describes the ratio of formed SOA and initial organic mass, for the variation of the particle radius r_p using a constant $k_c = 1 \text{ s}^{-1}$ (case 4a and 4b of Table 1); for a) liquid ($D_b = 10^{-12} \text{ m}^2 \text{ s}^{-1}$) and b) semi-solid ($D_b = 10^{-18} \text{ m}^2 \text{ s}^{-1}$) aerosol particles.

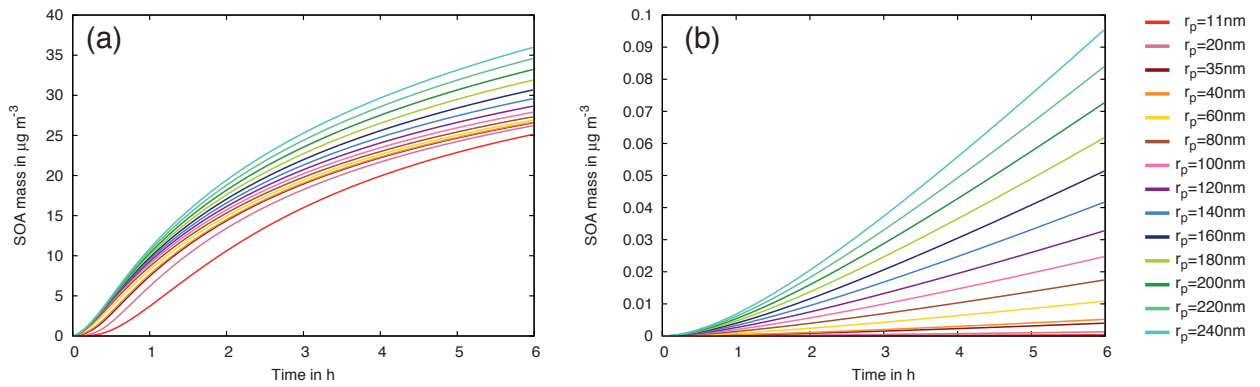


Figure S5. Results for the variation of the particle radius r_p for a constant $k_c = 10^{-4} \text{ s}^{-1}$ (case 4b of Table 1) for a) liquid ($D_b = 10^{-12} \text{ m}^2 \text{ s}^{-1}$) and b) semi-solid ($D_b = 10^{-18} \text{ m}^2 \text{ s}^{-1}$) aerosol particles.

2.5 Impact of different HOM vapor pressure estimates on SOA formation

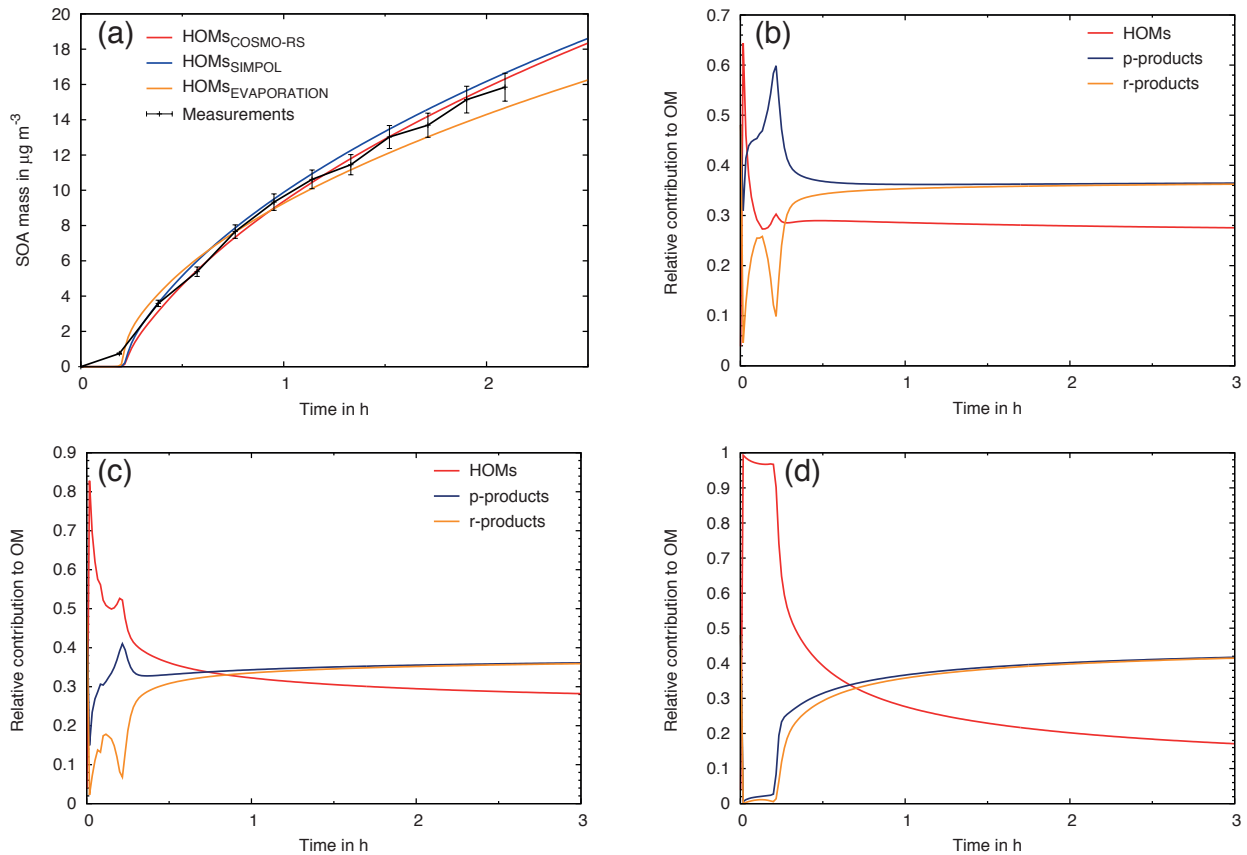


Figure S6. Results for the different vapor pressure estimates a) total SOA mass simulated with vapor pressure estimates from COSMO-RS (Eckert and Klamt, 2002), SIMPOL (Pankow and Asher, 2008) and EVAPORATION (Compernolle et al., 2011) and measured SOA mass from the experiment in LEAK. Relative contribution of the individual product classes to the total organic mass for HOM vapor pressures estimated by b) COSMO-RS c) SIMPOL d) EVAPORATION.

References

- Arey, J., Aschmann, S. M., Kwok, E. S. C., , and Atkinson, R.: Alkyl Nitrate, Hydroxyalkyl Nitrate, and Hydroxycarbonyl Formation from the NO_x-Air Photooxidations of C5-C8 n-Alkanes, *The Journal of Physical Chemistry A*, 105, 1020 – 1027, doi:10.1021/jp003292z, 2001.
- Atkinson, R.: Gas-Phase Tropospheric Chemistry of Volatile Organic Compounds: 1. Alkanes and Alkenes, *Journal of Physical and Chemical Reference Data*, 26, 215 – 290, doi:10.1063/1.556012, 1997.
- Berndt, T., Richters, S., Jokinen, T., Hyttinen, N., Kurtén, T., Otkjær, R. V., Kjaergaard, H. G., Stratmann, F., Herrmann, H., Sipilä, M., Kulmala, M., and Ehn, M.: Hydroxyl radical-induced formation of highly oxidized organic compounds, *Nature Communications*, 7, doi:10.1038/ncomms13677, 2016.
- Chen, J. and Griffin, R. J.: Modeling secondary organic aerosol formation from oxidation of α -pinene, β -pinene, and d-limonene, *Atmospheric Environment*, 39, 7731 – 7744, doi:10.1016/j.atmosenv.2005.05.049, 2005.
- Compernolle, S., Ceulemans, K., and Müller, J.-F.: EVAPORATION: a new vapour pressure estimation methodfor organic molecules including non-additivity and intramolecular interactions, *Atmospheric Chemistry and Physics*, 11, 9431 – 9450, doi:10.5194/acp-11-9431-2011, 2011.
- Davidovits, P., Kolb, C. E., Williams, L. R., Jayne, J. T., and Worsnop, D. R.: Mass Accommodation and Chemical Reactions at Gas-Liquid Interfaces, *Chemical Reviews*, 106, 1323 – 1354, doi:10.1021/cr040366k, 2006.
- Eckert, F. and Klamt, A.: Fast solvent screening via quantum chemistry: COSMO-RS approach, *AIChE Journal*, 48, doi:10.1002/aic.690480220, 2002.
- Glasius, M., Calogirou, A., Jensen, N. R., Hjorth, J., and Nielsen, C. J.: Kinetic study of gas-phase reactions of pinonaldehyde and structurally related compounds, *International Journal of Chemical Kinetics*, 29, 527 – 533, doi:10.1002/(SICI)1097-4601(1997)29:7<527::AID-KIN7>3.0.CO;2-W, 1997.
- Griffin, R. J., Dabdub, D., and Seinfeld, J. H.: Secondary organic aerosol 1. Atmospheric chemical mechanism for production of molecular constituents, *Journal of Geophysical Research: Atmospheres*, 107, 1 – 26, doi:10.1029/2001jd000541, 2002.
- Jenkin, M. E., Saunders, S. M., and Pilling, M. J.: The tropospheric degradation of volatile organic compounds: a protocol for mechanism development, *Atmospheric Environment*, 31, 81 – 104, doi:10.1016/s1352-2310(96)00105-7, 1997.
- Julin, J., Winkler, P. M., Donahue, N. M., Wagner, P. E., and Riipinen, I.: Near-Unity Mass Accommodation Coefficient of Organic Molecules of Varying Structure, *Environmental Science & Technology*, 48, 12 083 – 12 089, doi:10.1021/es501816h, 2014.
- Kwok, E. S. and Atkinson, R.: Estimation of hydroxyl radical reaction rate constants for gas-phase organic compounds using a structure-reactivity relationship: An update, *Atmospheric Environment*, 29, 1685 – 1695, doi:10.1016/1352-2310(95)00069-B, 1995.
- Pankow, J. F. and Asher, W. E.: SIMPOL.1: a simple group contribution method for predicting vapor pressures and enthalpies of vaporization of multifunctional organic compounds, *Atmospheric Chemistry and Physics*, 8, 2773 – 2796, doi:10.5194/acp-8-2773-2008, 2008.
- Saleh, R., Khlystov, A., and Shihadeh, A.: Determination of Evaporation Coefficients of Ambient and Laboratory-Generated Semivolatile Organic Aerosols from Phase Equilibration Kinetics in a Thermodenuder, *Aerosol Science and Technology*, 46, 22 – 30, doi:10.1080/02786826.2011.602762, 2012.
- Saunders, S. M., Jenkin, M. E., Derwent, R. G., and Pilling, M. J.: Protocol for the development of the Master Chemical Mechanism, MCM v3 (Part A): tropospheric degradation of non-aromatic volatile organic compounds, *Atmospheric Chemistry and Physics*, 3, 161 – 180, doi:10.5194/acp-3-161-2003, 2003.

Seinfeld, J. H. and Pandis, S. N.: Atmospheric Chemistry and Physics: from Air Pollution to Climate Change, 2nd Edition, John Wiley, New York, doi:10.1029/2007JD009735, 2006.